表2　ISO/TC 150「外科用インプラント」の構成

WG	Title	議長(国籍)	事務局	日本の参加状況
TC150	Implants for surgery(外科用インプラント)	USA	Germany	P-member
7	Fundamental standards(基本標準)			
8	Breast implants(人工乳房)			
10	Use and retrieval of surgical implants(外科用インプラントの使用と抜去)			
12	Implant coating(インプラントへのコーティング)			
SC1	Materials(材料)	UK	Germany	P-member
3	Ceramics(セラミックス)			
4	Metals(金属)			
5	Plastics(プラスチック)			
SC2	Cardiovascular implants and extracorporeal systems (心臓血管用インプラントおよび体外循環システム)	USA	USA	P-member
1	Cardiac valves(心臓弁)			
3	Vascular prostheses(人工血管)			
4	Blood gas exchangers(血液-ガス交換器(人工肺))			
5	Renal replacement, detoxification and apheresis(人工透析器)			
6	Vascular device/drug combination products (血管用機器ー薬剤コンビネーション製品)			
7	Cardiovascular absorbable implants(心臓血管用吸収性インプラント)			
SC3	Neurosurgical implants(神経外科用インプラント:休止中)	Germany	Germany	不参加
SC4	Bone and joint replacements(人工骨および人工関節)	UK	UK	P-member
1	Mechanical testing(力学試験)			
3	Wear(摩耗)			
4	General requirements(一般的要求事項)			
SC5	Osteosynthesis and spinal devices(骨接合機器および脊椎用機器)			
1	Osteosynthesis(骨接合機器)			
2	Spinal devices(脊椎用機器)			
SC6	Active implants(能動型インプラント)	Canada	USA	P-member
	Fundamental standards(基本標準)			
1	Cochlear implants(人工内耳)			
3	Implantable infusion pumps(植込み式輸液ポンプ)			
4	Implantable neurostimulators(植込み式神経刺激装置)			
5	Circulatory support devices(補助人工心臓)			
6	Cardiac pacemakers and implantable defibrillators (ペースメーカーおよび植込み式除細動器)			
JWG 1 (with IEC SC 62D)	Effects of magnetic resonance imaging on active implantable medical devices			
JWG 2 (with IEC SC 62B)	(MRIによる能動型インプラントへの影響)			
SC7	Tissue-engineered medical products(再生医療機器)	USA	Japan	P-member (事務局)
1	Management of risk(リスクマネジメント)			
2	General guideline of safety test(安全性試験の一般的ガイドライン)			
3	Tissue-engineered medical products for skeletal tissues (骨格組織用再生医療機器)			

WG: working group

・ ISO 5834-1:2005 Implants for surgery—Ultra-high-molecular-weight polyethylene—Part 1: Powder form

・ ISO 13179-1:2014 Implants for surgery—*In vitro* evaluation for apatite-forming ability of implant materials

・ ISO/TS 17137:2014 Cardiovascular implants and extracorporeal systems—Cardiovascular absorbable implants

【試験標準例】

・ ISO 7206-6:2013 Implants for surgery—Partial and total hip joint prostheses—Part 6: Endurance properties testing and performance requirements of neck region of stemmed femoral components

・ ISO 12891-2:2014 Retrieval and analysis of surgical implants—Part 2: Analysis of retrieved surgical implants

・ ISO 17853:2013 Wear of implant materials—Polymer and metal wear particles—Isolation and characterization

・ ISO 23317:2014 Implants for surgery—*In vitro* evaluation for apatite-forming ability of implant

表3　ISO/TC 194「医療機器の生物学的及び臨床評価」の構成

WG	Title	議長(国籍)	事務局	日本の参加状況
TC 194	Biological and clinical evaluation of medical devices (医療機器の生物学的および臨床評価)	Germany	Germany	P-member
1	Systematic approach to biological evaluation and terminology (生物学的評価における体系的な取組みと用語集)			
2	Degradation aspects related to biological testing (生物学的試験における材料分解性状に関する留意点)			
3	Animal protection aspects(動物愛護に関する留意点)			
4	Clinical investigations of medical devices in humans (医療機器の臨床試験)			
5	Cytotoxicity(細胞毒性)			
6	Mutagenicity, carcinogenicity and reproductive toxicity (変異原性,発がん性および生殖毒性)			
7	Systemic toxicity(全身毒性)			
8	Irritation, sensitization(刺激性,感作性)			
9	Effect on blood(血液への影響)			
10	Implantation(埋植試験)			
11	Allowable limits for leachable substances(溶出物の許容限界)			
12	Sample preparation and reference materials(試料調製と対照物質)			
13	Toxicokinetics(毒物動態学)			
14	Material characterization(材料特性評価)			
15	Strategic approach to biological assessment (生物学的アセスメントにおける戦略的取組み)			
16	Pyrogenicity(発熱性)			
17	Nanomaterials(ナノマテリアル)			
SC 1	Tissue product safety(組織由来製品の安全性)	USA	Germany	P-member
1	Risk assessment, terminology and global aspects (リスクアセスメント,用語集およびその他の事項)			
2	Sourcing controls, collection and handling (原料の制限,入手および処理)			
3	Elimination and /or inactivation of viruses and TSE agents (ウイルスおよびTSE原因物質の除去と不活化)			
4	TSE Elimination(TSE原因物質の除去)			

materials

これらのタイトルから，このTCにおける標準化の具体的な対象，さらにはみずからの研究成果や技術を当該TCにおいて標準化する手段が存在することを，本稿の読者には理解していただけることを期待する．ただし，みずからの技術を標準化する最終目標は，標準化自体ではなく，それを用いた医療機器が数多く開発され上市化されることであることに留意されたい．特に，このTCのように個別の材料・製品に特化した標準を作成する場合は，さらなる技術発展の阻害にならないよう適切な標準化戦略が必要となる．

2.TC 194 Biological and clinical evaluation of medical devices (医療機器の生物学的および臨床評価)

1988年に設立されたTCであり，医用材料および医療機器の安全性に関する生物学的評価方法(細胞毒性，変異原性，全身毒性等)と臨床試験基準(GCP)に関する標準化を討議してきている．このTCで作成されている生物学的評価に関する標準は，その番号からISO 10993シリーズとして医療機器業界に知られており，特にWG 1で作成された基本的考え方に関する標準は国内通知[3]にも引用されている．

材料が人体に障害を引き起こす原因は，材料と接触した血液や組織液に溶出する化学物質の毒性に由来することが多い．現在，医療機器の安全性評価を行うにあたっては，毒性の原因となりうるハザードの特定，特定されたハザードによるリスクの推定等が，JIS T 14971「医療機器—リスクマネジメントの医療機器への適用」に示されたリスク分析手法を用いて実施されなければならない．その後，実際に使用される状況に応じたリスク解析を行うことにより，医療機器の生物学的安全性が評価される．

材料によって生体が受ける障害は，炎症，アレルギー，発熱，組織壊死，腫瘍等の形で出現するため，各毒性反応を検出しうる生物学的試験を用いてそれらの安全性を評価する．個々の医療機器の生物学的安全性評価に求められる試験項目は，実際に使用さ

れる状況，具体的には，医療機器のカテゴリー，接触部位，接触期間に応じて選択する必要がある．そのための基本的な考え方はこのTCで作成されたISO 10993-1に記載されており，上述したように国内通知にも引用されている．TC 150で数多く作成されている個別標準と異なり，このTCで作成されたISOはほとんどの医療機器に適用されうるホリゾンタルな標準であり，医療機器業界における重要性は大きい．

現存するWGは17，SCは1であり，そのSCは四つのWGをもつ(表3)．なお，SC 1は2008年にScopeを変更し，親TCでは対象とされていない生きた組織，すなわち細胞等の安全性に関する事柄も扱うことになり，2013年には，このSCで討議された「生きたヒト細胞を含む医療製品のリスクマネジメント」に関する標準(ISO 13022:2012)が発行された．これは，ISOにおいて発行された最初の再生医療関係の標準である．このTCで発行した標準はこれまでに30存在し，その多くが国内外の規制に引用されている．具体的な標準の内容，現在の討議事項に関して興味のある方は，ISOのホームページ[4]や弊部に開設しているTC 194国内委員会ホームページ[5]をご覧いただきたい．

近年の活動で特筆すべき事項は，国内委員会主催で開催されたTC 194年次総会(2014年4月，三島市)において，体内吸収性材料に関する考え方や試験法に加え，動物愛護の高まりに伴う動物試験削減のための考え方を標準に追加することが参加者間の活発な討議により合意され，当該TCがこれまでに作成したほとんどすべての標準の改訂作業を開始するに至ったことである．また，一部WGでは，各国で開発された新規の安全性評価技術を標準に取り込むための作業も開始することになった．このことから分かるように，必要とされる標準は，その時代に応じた形に修正されていくものであり，そのためのバックグラウンドデータを得るための材料や試験法に関する継続的かつ地道な基礎的研究が必要となる．その一方で，新規材料の開発においては，これらの標準に記載された試験法により生物学的安全性を評価することが求められるため，最先端の研究を行っている研究者であってもこのTCの活動や発行されたISOを無視することはできない．

歴史的に，日本はTC 194設立当時からのP-memberであり，初期の実質的な審議主体は本学会であったことが国内委員会ホームページ議事録に掲載されている．その議事録には，1995年に国内の生物試験法ガイドラインが通知として発出され，TC 194も試験の枠組みと個別試験法の一通りの標準化作業を終えたことから，改訂や問題点解決等，以降に必要とされる作業の主体を企業および規制当局に移行させるべきであるとの判断が当時の審議メンバーによりなされ，1997年をもって本学会はTC 194の討議から距離をおくことになったとの記載があった．この時点で本学会とTC 194との直接的な関係はなくなったが，標準作成作業では一定の科学的知識を有するメンバーでの討議が必須であるため，必然的に各国からは規制関係者や企業関係者，コンサルタントらに加え科学者，特にバイオマテリアル研究者がメンバーとして推薦されることになる．

日本においても，筆者らを含め，現在のTC 194国内委員会メンバーの多くが本学会員であることから，いまだにTC 194と本学会との関係はある程度の距離を保ちながらつづいているといってよい．上述したように，本TCの活動はバイオマテリアルの実用化に大きく影響するため，今後，学会および学会員の皆様の積極的な関与をお願いしたい．

医療機器関連国際標準化支援窓口の試験的開設

筆者らは，平成23, 24年度に行った厚生労働科学研究費補助金事業において「医療機器規格・基準の国際標準化戦略に係る政策的提言」を作成し，日本発の医療機器を国際的に進出させるための環境整備における国際標準化推進の重要性を提言した．当該提言に含まれる施策は多岐にわたり，その一項目として米国のAmerican National Standards Institute(ANSI)，英国のBritish Standards Institution(BSI)，ドイツのDeutsches Institut für Normung(DIN)のように，自国政府および関連省庁と連携して基礎データの収集や保持管理も行いつつ国際標準化活動を分野毎にとりまとめ，一元的かつ戦略的に実施・サポートする機関を国内に設立する必要性が指摘されている．この

提言をもとに，本年度から，厚生労働科学研究費補助金事業により，医療機器の標準化に関する情報を一元的に収集してとりまとめて発信するための試験的窓口を弊部ホームページ[6]に設立した．表1にあげたように，医療機器に関連したISOおよびIECのTCは非常に多く，また発行された標準の総数も千を超え，限られた人員ですべての医療機器を対象とした作業を行うことは不可能なことから，まずは注目度の高い医療機器に対象を絞り，関連したTCやSCの活動状況を調査し取りまとめることにした．

調査対象として選択した製品は，「再生医療等製品」と「医療機器ソフトウェア」であり，いずれも，近年，急速に発展し，今後もその展開が着目されている分野である．昨年11月より「再生医療等製品」は，医療機器とは別の枠組みで規制されており，厳密には医療機器ではない．しかし，多くの再生医療等製品にはバイオマテリアルが使用されており，その安全性・有効性においては細胞および医用材料との相互作用解析が重要となる．また，筆者の一人が当該製品の国際標準化に関わっていることから調査対象分野として選定した．後者は，stand aloneの医療用ソフトウェアであってもその用途によって規制対象となったことから，従来以上に関連する国際標準が安全性や品質を検討するうえで重要となるため調査対象とした．ホームページは未完成であり，2014年11月現在は再生医療機器の状況のみを公開しているが，本稿が「バイオマテリアル」誌に掲載されるころには，その更新とソフトウェアの標準化に関する情報を公開できるよう努力したい．

この活動を通して明確になった特筆すべき事項は，国際標準化に積極的な企業が少ないこと，関与している企業においてもその担当者への特別なサポート等がほとんどなく，担当者は正当な評価を受けていないと感じていることなど，多くの企業が国際標準化の重要性を理解していないことである．具体的には，事業における標準化と知的財産権との戦略的な使い分けを行っていないとともに，知的財産権の確保のみで市場を勝ち抜く，旧態の事業戦略から脱却していない企業が数多く存在することが判明した．このような現状を打破するためには，医療機器関連の研究者のみならず，企業経営陣を対象とした国際標準化の啓蒙活動が必要であることも明らかとなった．前述した「健康・医療戦略」に医薬品，医療機器等の審査において利用可能な国際標準化の策定，提案等の推進が国策として明記された状況を鑑みると，このような状況は医療機器開発に携わるすべての関係者にとって好ましくない．

筆者らは，今後も医療機器開発に携わる産･官･学関係者を対象とした啓蒙活動を行っていく予定であるが，本稿により標準化の重要性を理解していただいた読者の方々には，ぜひともみずからの研究に関係するTCの活動にご協力いただくとともに，ご自分の技術を含めたわが国発の医療機器標準作成への積極的な関与をお願いしたい．なお，関連TCへの橋渡しを担当させていただくことも可能であるため，標準化活動にご興味をもたれた読者の方々は筆者らにご一報いただきたい．少なくとも本稿により，読者にとって医療機器関連の国際標準化に関する理解を深めるきっかけになると同時に，わが国発の国際標準作成の活性化，さらにはそれを通じた医療機器国際市場の新規開拓等の国内産業活性化ならびに医療機器審査の迅速化等への取り組み状況を理解するための一助になれば幸いである．

本稿に紹介した活動および研究成果の一部は，厚生労働科学研究費補助金地球規模保健課題事業「医療機器規格の国際標準化を支援する体制構築に関する研究」による．

文　献

1) http://www.kantei.go.jp/jp/singi/kenkouiryou/suisin/ketteisiryou/dai2/siryou1.pdf
2) http://www.jisc.go.jp/international/index.html
3) 平成24年3月1日付薬食機発0301第20号厚生労働省医薬食品局審査管理課医療機器審査管理室長通知「医療機器の製造販売承認申請等に必要な生物学的安全性評価の基本的考え方について」(http://www.pmda.go.jp/kijunsakusei/file/guideline/medical_device/T120302I0070.pdf)
4) http://www.iso.org/iso/home/standards_development/list_of_iso_technical_committees/iso_technical_committee.htm?commid=54508
5) http://dmd.nihs.go.jp/iso-tc194/index.html
6) http://dmd.nihs.go.jp/chikyukibo/index.html

Ⅲ．研究成果の刊行に関する資料③

Dental Materials Journal,33:422-429 (2014)

Dental Materials Journal 2014; 33(3): 422–429

A new method for fabricating zirconia copings using a Nd:YVO_4 nanosecond laser

Miku KAZAMA-KOIDE[1], Kazuo OHKUMA[2], Hideo OGURA[3] and Yukio MIYAGAWA[1,2]

[1] Developmental Science of Oral Biomaterials, The Nippon Dental University Graduate School of Life Dentistry at Niigata, 1-8 Hamaura-cho, Chuo-ku, Niigata 951-8580, Japan
[2] Department of Dental Materials Science, The Nippon Dental University School of Life Dentistry at Niigata, 1-8 Hamaura-cho, Chuo-ku, Niigata 951-8580, Japan
[3] The Nippon Dental University, 1-9-20 Fujimi, Chiyoda-ku, Tokyo 102-8159, Japan
Corresponding author, Miku KAZAMA-KOIDE; E-mail: miku@ngt.ndu.ac.jp

The purpose of this work was to fabricate zirconia copings from fully sintered Y-TZP blocks using a Nd:YVO_4 nanosecond laser in order to avoid complicated procedures using conventional CAD/CAM systems. To determine the most appropriate power level of a Nd:YVO_4 laser, cuboid fully sintered Y-TZP specimens were irradiated at six different average power levels. One-way ANOVAs for the average surface roughness and laser machining depth revealed that an average power level of 7.5 W generated a smooth machined surface with high machining efficiency. Y-TZP copings were then machined using the proposed method with the most appropriate power level. As the number of machining iterations increased, the convergence angles decreased significantly ($p<0.01$). The accuracy of the machined copings was judged to be good based on 3D measurements and traditional metal die methods. The proposed method using the nanosecond laser was demonstrated to be useful for fabricating copings from fully sintered Y-TZP.

Keywords: Y-TZP, CAD/CAM, Zirconia, Laser, Nd:YVO_4

INTRODUCTION

Recently, dentists and patients have become interested in all-ceramic restorations, which do not contain metals, which block light transmission, and better resemble the natural tooth appearance than any other restorative option[1]. In addition, all-ceramic restorations do not cause metal allergy problems. The clinical shortcomings of ceramic materials, such as brittleness, low tensile strength, and marginal inaccuracy, continue to limit their use compared to porcelain-fused-to-metal crowns[2,3]. Nevertheless, patients' demand for improved esthetics has driven the development of ceramic restorations. The use of all-ceramic restorations has spread as a result of the application of high-strength ceramics, such as zirconia, to the coping materials.

Zirconia ceramics for dental restorations have high strength and high toughness, which allows these materials to be used as all-ceramic coping materials for long-span bridges. However, machining fully sintered zirconia by milling is very difficult because of its high hardness. The coping is fabricated with an established method using a CAD/CAM system in which a partially sintered zirconia block is milled and subsequently sintered in a furnace. A linear shrinkage of 15 to 30% occurs due to sintering[4]. The increased milling efficiency of the softer partially sintered block has the trade-off of a potentially poorer fit caused by the sintering shrinkage, the scanning process, compensatory software design, and milling[5]. In order to avoid these complicated procedures, we have devised a new simple method by which to machine high-hardness zirconia using a laser. A range of lasers is now available in dentistry. The Nd:YAG laser can be used in the dental laboratory for laser welding. Metal parts such as frameworks can be joined by self-welding of the parts with combustible acrylic denture base resins and artificial composite teeth, which would be burned by conventional soldering[6]. Noda *et al.* conducted an experiment involving the irradiation of zirconia using this Nd:YAG laser and examined the possibility of welding zirconia[7]. They reported that laser irradiation induced cracking on the surfaces of zirconia so Nd:YAG dental laser welding should not be performed on zirconia[7]. Nd:YAG dental laser irradiation, which produced a millisecond-order pulse width, generated thermal effects on zirconia[8].

Therefore, we devised a new method by which to machine zirconia copings using an industrial Nd:YVO_4 Q-switched nanosecond laser, which had a smaller pulse width and a power density that was several hundred times higher than that of the conventional Nd:YAG dental laser. The purpose of the present study was to demonstrate the possibility of Nd:YVO_4 Q-switched nanosecond laser machining of zirconia copings.

MATERIALS AND METHODS

Nd:YVO_4 laser machine

In the present study, fully sintered yttria-stabilized tetragonal zirconia polycrystal (Y-TZP) specimens were machined using a Q-switched Nd:YVO_4 (Neodymium Doped Yttrium Vanadate) laser machine (Lasertec 40, DMG, Berlin, Germany, Fig. 1) for fabricating the Y-TZP copings of all-ceramic restorations. This nanosecond laser machine generated a power density of 2.26×10^4 (kW/mm^3), which is several hundred times higher than

Received Dec 13, 2013: Accepted Mar 12, 2014
doi:10.4012/dmj.2013-348 JOI JST.JSTAGE/dmj/2013-348

Fig. 1 $Nd:YVO_4$ laser machine.

a dental Nd:YAG laser with a millisecond pulse. The fundamental parameters of the $Nd:YVO_4$ laser machine are listed in Table 1.

Fully sintered yttria-stabilized tetragonal zirconia polycrystals (Y-TZP)

Two types of fully sintered Y-TZP specimens were prepared as follows. The discs of partially sintered Y-TZP (height: 25 mm, diameter: 98.5 mm, Aadva Zr disk, GC, Tokyo, Japan) were milled and subsequently sintered at 1,550°C for 18.5 h in a furnace using a dental CAD/CAM system (GM-1000, GC, Tokyo, Japan). Partially sintered Y-TZP consisted of >91 wt% ZrO_2, 5 wt% Y_2O_3, <3 wt% HfO_2, and <1 wt% Al_2O_3.

One cuboid (13 mm×13 mm×17 mm) fully sintered Y-TZP specimen was used to determine the most appropriate power level of the $Nd:YVO_4$ laser irradiation condition for fully sintered Y-TZP and another specimen (height: 7 mm, baseline: 10.6 mm), as shown in Fig. 2, was machined to form a Y-TZP coping on an abutment tooth of an imitation lower first molar.

Determination of the most appropriate power level of the $Nd:YVO_4$ laser

In order to determine the most appropriate power level of the $Nd:YVO_4$ laser, a cuboid fully sintered Y-TZP specimen was irradiated at six different average power levels (3, 6, 7.5, 9, 12, and 14 W). The irradiated surface area was square (2 mm×2 mm). The specimen was cleaned in distilled water using an ultrasonic cleaner. The machining depth and the calculated average roughness (Ra in μm) at each of the six power levels were evaluated. The machining depth was measured using a measuring microscope (STM6, OLYMPUS, Tokyo, Japan). The calculated average roughness was also measured using a laser microscope (VK-8500, KEYENCE, Osaka, Japan) with a cut off value of 0.8 mm. One-way ANOVA and Tukey's multiple comparison test were used to analyze the data.

Table 1 Specifications of the laser machine

Specification	Description
Laser type	$Nd:YVO_4$ crystal
Wave length	1,064 nm
Pulse width	18 ns
Operation mode	Q switched pulse
Scan speed	500 mm/s
Peak power	16 kW
Pulse frequency	50 kHz
Focus diameter	30 μm
Track distance	10 μm

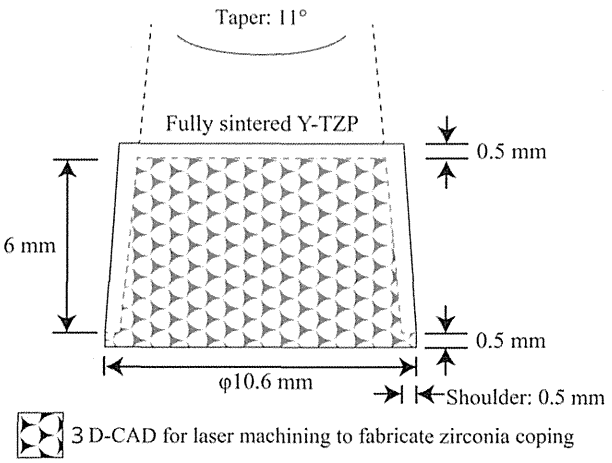

Fig. 2 Dimensions of the fully sintered Y-TZP specimen simulating a lower first molar, and 3D-CAD for laser machining to fabricate zirconia coping.

Machining Y-TZP copings using the $Nd:YVO_4$ laser machine

Machining 3D-CAD data of a Y-TZP coping were constructed using CAD software (Rhinoceros4.0, Robert McNeel & Associates, WA, USA). Y-TZP copings were machined in order to create the final form with a convergence angle of 11°, a cervical width of 10.6 mm, and a shoulder part width of 0.5 mm using 3D-CAD data (Fig. 2). The part that touched the abutment tooth, as shown in Fig. 2, was machined. Y-TZP copings were fabricated from fully sintered blocks using the $Nd:YVO_4$ laser machine with an optimal machining condition

(n=6). Machining each coping required eight hours. Y-TZP copings were machined in 100-μm increments, as measured using calipers integrated into the laser machine for depth control. At first machining, the machining residue in the width direction of Y-TZP coping occurred on the inner surface so that the convergence angle of coping was greater than 11°, as designed based on machining 3D-CAD data. Therefore, the coping was machined two, three, or four times until the machining residue disappeared (Fig. 3).

Machining accuracy

1. Evaluation of machining accuracy by 3D measurement

Machined Y-TZP copings were measured using a non-destructive industrial 3D scanner (ATOS I 2M, GOM mbH, Brunswick, Germany) at every machining, and 3D-CAD data of copings were constructed. Dimensional differences in the height direction and width direction between the 3D-CAD data for machined Y-TZP copings and the target 3D-CAD data of Y-TZP copings were inspected using inspection software (GOM inspect, GOM mbH, Brunswick, Germany). Twelve measurement points were set in the width direction: 0, 0.5, 1, 1.5, 2, 2.5, 3, 3.5, 4, 4.5, 5, and 5.5 mm away from the inner cervical line of the Y-TZP coping (Fig. 4). In the height direction, six measurement points were set: −3, −2, −1, 0, 1, 2, and 3 mm away from the occlusal center of Y-TZP coping (Fig. 4). The results for the dimensional differences in the width direction and the machining frequency were analyzed by two-way repeated-measures ANOVA and Sidak's multiple comparison test. One-way repeated-measures ANOVA and Sidak's multiple comparison test were used to analyze the results for the dimensional differences in the height direction. The convergence angle of the inner coping was measured at each machining. One-way repeated measures ANOVA and Sidak's multiple comparison test were used for analyzing the results of the convergence angle of inner-machined copings.

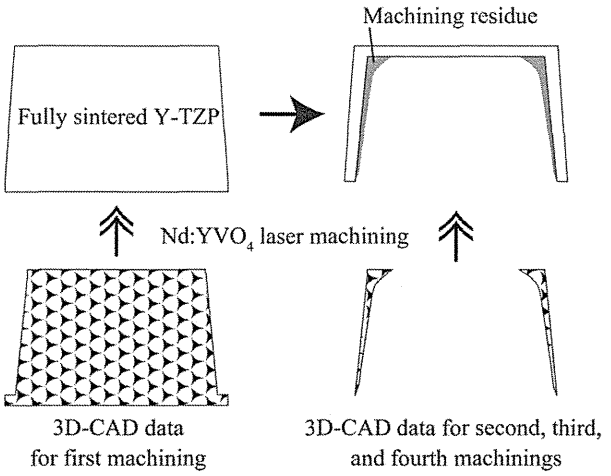

Fig. 3 Method of fabricating a zirconia coping having an inner taper of 11° and a cervical width of 9.6 mm.

2. Evaluation of machining accuracy using metal dies

Machined copings at the fourth machining were measured using dies having different cervical widths of 9.60 mm (Abutment 1), 9.58 mm (Abutment 2), and 9.56 mm (Abutment 3). The convergence angle of each die was 11°. Y-TZP copings were placed on the metal die (Fig. 5) without cementation, and the marginal discrepancy (L-L1) was measured using a measuring microscope (STM6, OLYMPUS, Tokyo, Japan). Negative values for L-L1 indicate that copings were machined smaller than the machining CAD, whereas positive numbers indicate that the copings were machined larger than the machining CAD (Fig. 5). One-way ANOVA and Sidak's multiple comparison test were used to analyze the results for the goodness of fit.

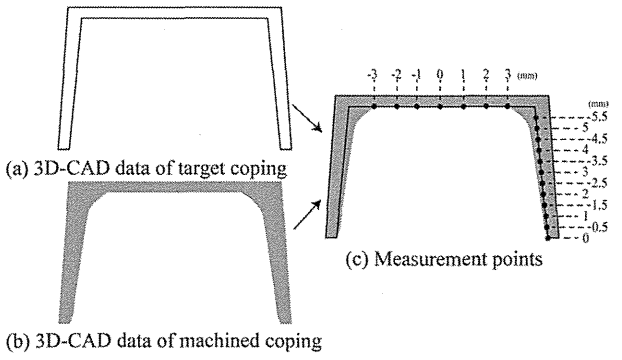

Fig. 4 Schematic diagrams of 3D measurement for machining accuracy.
The dimensional differences between (a) and (b) were inspected using inspection software. (c) Measurement points in the height and width directions.

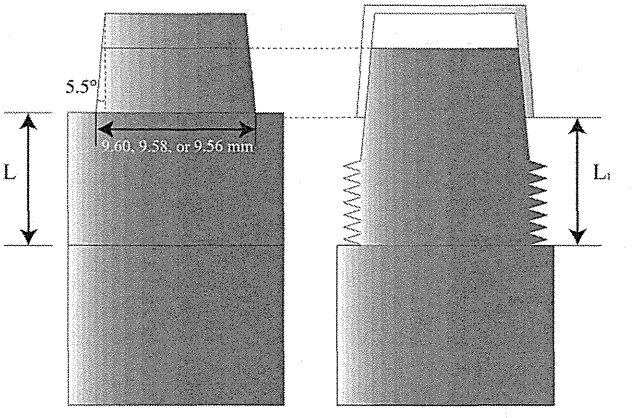

Fig. 5 Schematic diagrams of a metal die having a taper of 11° used to evaluate machining accuracy.

RESULTS

Determination of the most appropriate power level of the Nd:YVO$_4$ laser

The means and standard deviations (SD) of the calculated average roughnesses (Ra) and the machining depths of the irradiated Y-TZP surfaces are shown in Table 2 and Fig. 6.

The values of Ra for average powers of 6 W, 7.5 W, and 9 W were smaller than those for average powers of 3 W and 12 W, and the values of Ra for average powers of 6 W and 7.5 W were smaller than that for an average power of 14 W ($p<0.05$). Therefore, the Y-TZP surface was machined to be the smoothest at 6 W and 7.5 W using the Nd:YVO$_4$ laser. As the average power increased, the machining depth tended to increase, but became smaller from 12 W to 14 W. The machining depths per pulse for average powers of 7.5 W, 9 W, 12 W, and 14 W were greater than that for an average power of 3 W ($p<0.05$), and machining depth per pulse for an average power of 12 W was greater than that for an average power of 6 W ($p<0.05$). When the above analysis results for the calculated average roughness and the machining depth were put together, the average power level of 7.5 W, at which the smoothest Y-TZP surface could be obtained with high machining efficiency, was decided to be the most appropriate power level.

Table 2 Average roughness and machining depth per pulse after nanosecond laser irradiation of fully sintered Y-TZP

Average power (W)	Average roughness (Ra, μm)	Machining depth (μm)
	Mean (SD)	Mean (SD)
3	0.63 (0.11)	1.9 (1.4)
6	0.37 (0.06)	3.7 (0.4)
7.5	0.40 (0.05)	4.8 (0.5)
9	0.43 (0.02)	5.5 (0.6)
12	0.67 (0.07)	5.9 (0.6)
14	0.62 (0.07)	4.7 (0.2)

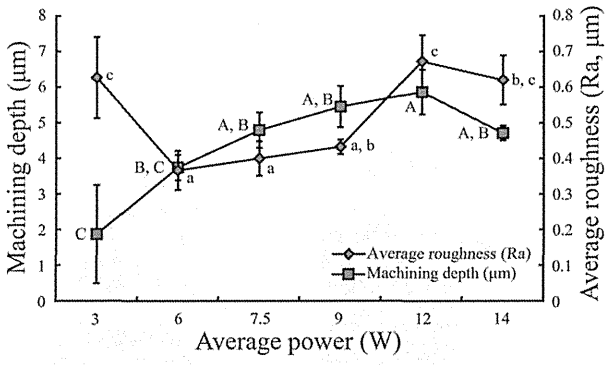

Fig. 6 Means and standard deviations of calculated average roughnesses (Ra) and machining depths of irradiated Y-TZP surfaces for different average power levels.
The six average power levels were statistically divided into three subgroups (a, b, and c) with respect to average roughness and three subgroups (A, B, and C) with respect to machining depth. Means with different letters are significantly different ($p<0.05$).

Machining Y-TZP copings using the Nd:YVO$_4$ laser machine

An optimal machining condition with an average power of 7.5 W was used to machine Y-TZP copings from fully sintered specimens. At first machining, machining residue was deposited in the width direction on the inner surface of the Y-TZP copings, so that the convergence angle was greater than 11°, which were designed as the machining 3D-CAD data (Fig. 3). The machining residue of Y-TZP copings was measured using an industrial 3D scanner, and the machining data were reacquired. The Y-TZP copings were then machined again using the new data. This process was repeated for the same Y-TZP coping until the fourth machining.

Machining accuracy

1) Machining accuracy using 3D measurement

Figure 7 and Table 3 show the dimensional difference in the height direction for a certain section between the CAD data of the machined Y-TZP copings and the target CAD data for the coping obtained through 3D measurement. The average dimensional difference in the height direction was 73.6 μm. Figure 8 and Table 4 show the dimensional difference in the width direction obtained using 3D measurement. Two-way repeated-

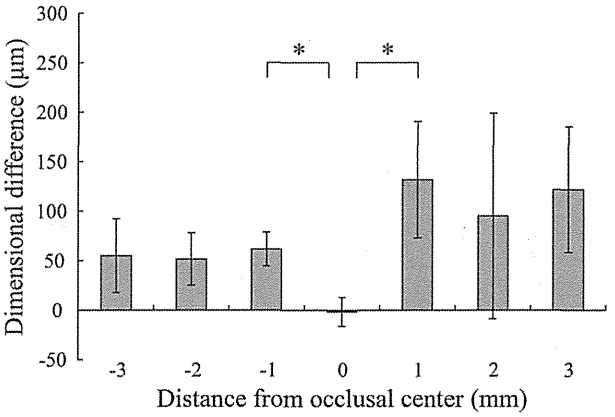

Fig. 7 Means and standard deviations of dimensional differences in the height direction.
The asterisk (*) indicates a significant difference at $p<0.05$.

Table 3 Dimensional difference in the height direction at each measurement point

Distance from occlusa. center (mm)	Dimensional difference (μm)	
	Mean	(SD)
−3.0	55.0	(37.3)
−2.0	51.7	(26.4)
−1.0	61.7	(17.2)
0.0	−1.7	(14.7)
1.0	131.7	(58.8)
2.0	95.0	(130.9)
3.0	121.7	(63.7)

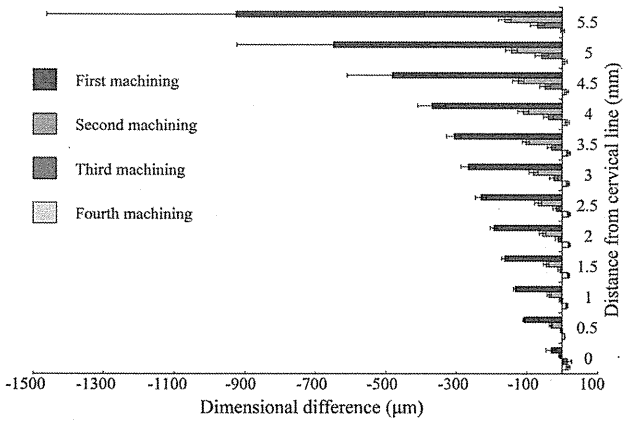

Fig. 8 Means and standard deviations of dimensional differences in the width direction.

measures ANOVA revealed that both main effects were significant ($p<0.01$). As shown in Fig. 8, the dimensional difference in the width direction decreased as the number of machining iterations increased and as the distance from the cervical line decreased, although the interaction between the two primary effects was also significant ($p<0.05$). The simple primary effect of the distance from the cervical line was not significant at the third or fourth machining ($p<0.05$). The dimensional difference in the width direction at the fourth machining was at most approximately 20 μm.

Figure 9 shows the inner convergence angle of machined copings of particular cross sections. The means and standard deviations, which are shown in parentheses, of the inner surface convergence angle were

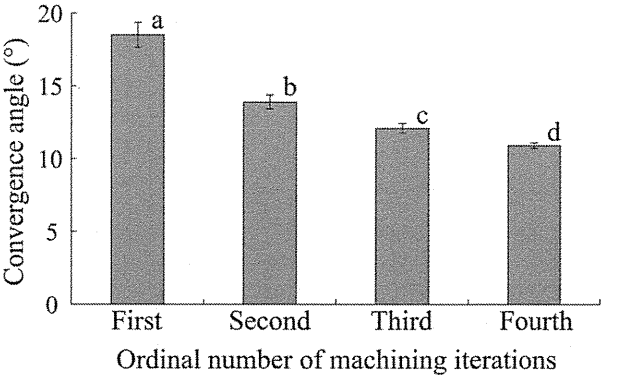

Fig. 9 Means and standard deviations of convergence angles of inner machined copings.
Means labeled with different letters (a, b, c, and d) are statistically different from each other ($p<0.01$).

Table 4 Dimensional difference in the width direction at each measurement point

Distance from cervical line (mm)	Dimensional difference (μm)							
	First machining		Second machining		Third machining		Fourth machining	
0.0	−30.1	(14.8)	−6.5	(3.0)	15.1	(12.0)	17.2	(5.0)
0.5	−107.5	(2.9)	−31.0	(4.7)	−1.9	(3.0)	7.6	(0.6)
1.0	−132.6	(4.6)	−36.3	(6.1)	−3.1	(4.4)	14.0	(2.8)
1.5	−161.9	(9.0)	−44.7	(8.3)	−6.0	(5.5)	18.2	(2.7)
2.0	−192.2	(10.9)	−55.3	(9.3)	−10.8	(8.0)	20.0	(2.4)
2.5	−229.2	(16.3)	−68.0	(10.4)	−16.7	(8.7)	19.1	(3.9)
3.0	−265.0	(21.4)	−81.1	(12.7)	−23.5	(12.0)	16.5	(4.2)
3.5	−305.6	(21.8)	−102.6	(10.3)	−30.0	(12.2)	17.8	(4.5)
4.0	−369.4	(40.1)	−110.6	(15.7)	−39.0	(14.1)	14.3	(5.8)
4.5	−481.8	(127.6)	−125.0	(16.4)	−48.2	(15.8)	11.5	(5.7)
5.0	−649.0	(274.6)	−143.9	(16.8)	−58.2	(19.4)	6.8	(6.9)
5.5	−926.4	(536.0)	−162.8	(17.9)	−70.6	(20.5)	1.8	(5.1)

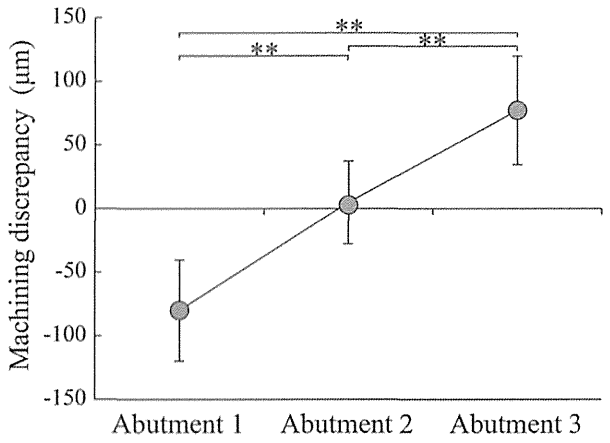

Fig. 10 Machining accuracy using three metal dies having convergence angles of 11° and different cervical widths; Abutment 1: 9.60 mm, Abutment 2: 9.58 mm, and Abutment 3: 9.56 mm. Significant differences are indicated by asterisks '**' ($p<0.01$).

determined to be as follows: 18.5° (0.86°) for the first machining, 13.9° (0.47°) for the second machining, 12.1° (0.34°) for the third machining, and 10.9° (0.18°) for the fourth machining. One-way repeated-measures ANOVA revealed that the number of machinings significantly affected the inner convergence angle of Y-TZP coping. As the number of machining iterations increased, the convergence angle decreased significantly ($p<0.01$). At the fourth machining, the convergence angle was comparable to the target 3D-CAD data.

2) Machining accuracy using the metal dies

The marginal fits of the Y-TZP copings that were machined four times were measured using metal dies. The means and standard deviations, which are shown in parentheses, of L-L1 were −80.2 (40.0) μm, 4.8 (32.6) μm, and 77.0 (42.0) μm using Abutments 1, 2, and 3, respectively. The larger the cervical width, the smaller the value of L-L1 (Fig. 10). The copings fit accurately on Abutment 2.

DISCUSSION

Determination of the most appropriate power level of the Nd:YVO$_4$ laser

The average roughness and machining depth were measured in order to determine the most appropriate average power level (W) of the Nd:YVO$_4$ laser on fully sintered Y-TZP. Excellent lasing performance on Y-TZP, which has high machining efficiency and provides a smooth surface, is most important. As shown in Fig. 6, the six average power levels considered herein were statistically divided into three subgroups (a, b, and c) with respect to average roughness and three subgroups (A, B, and C) with respect to machining depth. The average power level of 7.5 W belonged to both subgroup a (smallest average roughness) and subgroup A (greatest machining depth). Therefore, the average power level of 7.5 W, at which the smoothest Y-TZP surface could be obtained with high machining efficiency, was considered to be the most appropriate power level for the Nd:YVO$_4$ laser. High machining efficiency reduces the machining time.

Machining accuracy of Y-TZP copings

The copings, which were extracoronal restorations, were able to be machined from fully sintered Y-TZP using the nanosecond laser. Figure 7 shows that the dimensional difference in the height direction was not uniform. Air was blown from three directions on the Y-TZP coping in order to avoid reattachment of fine particles. However, locational differences were thought to occur as a result of the air being blown non-uniformly against the copings. Controlling the depth direction in machining (Z-axis) using a focused laser beam is generally difficult. Therefore, the copings were machined using an improved method for the depth control. In this experiment, the dimensional difference in the height direction was at most 132 μm for the planned 6.5 mm in the height direction based on machining CAD data, which gives an error of only 2.0%. In the width direction, the dimensional difference was at most 20 μm. The mean and standard deviation of the convergence angles of the inner copings were 10.9° and 0.18°, respectively.

In addition, the inside of the coping might be slightly oval-shaped. Therefore, in order to clinically evaluate the precision, a traditional experiment was conducted in which the dimensional accuracy was evaluated using a die method. We prepared three metal dies having different cervical widths. Since the machining 3D-CAD data (Fig. 2) did not take into account the cement layer or the coefficient of friction, the marginal discrepancy at the cervical line could not be obtained using Abutment 1, the cervical width of which was the same as in the machining 3D-CAD data. Therefore, dies having smaller cervical widths had to be used to measure the marginal discrepancy. The results revealed that the copings fit accurately on the die. The aforementioned discrepancies could be further improved by a slight modification of the design program of the CAD system. Marginal discrepancies of less than 120 μm have been reported to be clinically acceptable[9]. Thus, accurate machining of zirconia coping for clinical use using the Nd:YVO$_4$ laser is possible.

Laser machining of Y-TZP

At present, Y-TZP copings are fabricated using a dental CAD/CAM system in which a partially sintered Y-TZP block (12 HV) is milled and subsequently sintered in a furnace. Machining design can compensate for the approximately 20% volume shrinkage that occurs later during sintering of the zirconia blocks. Therefore, we devised a new method by which to machine a Y-TZP coping directly from a fully sintered Y-TZP block using an industrial Nd:YVO$_4$ Q-switched nanosecond

laser. The use of lasers to machine ceramics presents a number of advantages over the other methods. Laser machining is a noncontact technique that allows high-precision machining of numerous types of ceramics and eliminates tooling costs, which are expensive.

Generally, the material properties of Y-TZP, specifically its high thermal expansion coefficient (11×10^{-6}/°C) and low thermal conductivity (2 W/mK)[10], make laser machining of this material difficult. Due to the strong thermal nature of the laser beam-material interaction, especially in the case of long pulse widths, microcracks are generated by dental lasers, which generate millisecond-order pulse widths, as a result of thermal damage. In the present study, we used a nanosecond pulsed laser, which could significantly reduce thermal damage. The formation of cracks in the irradiated surface was seldom observed when using the nanosecond laser, and cracks that observed were extremely small, having depths of approximately 3 μm. Thus, the use of an ultrashort pulse laser that produces a picosecond pulsed laser or a femtosecond pulsed laser can significantly reduce the above-mentioned thermal effects, such as thermal damage or microcracks. However, such lasers require too much machining time to be adapted for practical application. Therefore, the potential of nanosecond laser machining on Y-TZP was demonstrated herein. Approximately 90% of the material removed through the proposed laser machining is a result of the interaction between the laser beam and the surface of the Y-TZP workpiece being machined. The nanosecond laser used is thus suitable for use in the machining of dental restorations.

The laser machine used herein provided three-axis machining, in which a Y-TZP specimen was irradiated from one direction (Z-axis). In addition, machining a hole with a convergence angle by condensing a laser beam has certain limitations because a focused laser produces a tapered hole. Accurately machined copings for clinical use were obtained after the fourth machining. On the other hand, a five-axis laser machine can instantly machine a taper-less hole because the laser beam can irradiate vertically with respect to the work piece[11]. In other words, a five-axis machine would provide the Y-TZP copings with improved retention and accuracy for clinical use and reduce costs by reducing the machining and finishing times.

Figure 11 shows a crown coping that was machined at an average power of 7.5 W. A dental restoration more complicated than the simple abutment coping shown in Fig. 2 was successfully machined from a fully sintered Y-TZP block, as shown in Fig. 11.

In comparison with a Nd:YAG laser, the Nd:YVO_4 laser has advantages such as the ability to produce more compact systems, because the Nd:YVO_4 crystal has 5 times higher absorption coefficient than Nd:YAG crystal. In addition to this, the laser has a higher efficiency thanks to a high stimulated emission cross section. A Nd:YVO_4 single crystal can be used for compact, high-efficiency machining, as compared with a Nd:YAG single crystal[12,13].

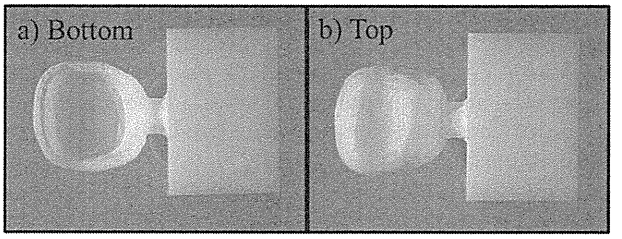

Fig. 11 A crown coping machined at an average power of 7.5 W.
The crown coping was successfully fabricated in a clinical form.

Darkening of the machined Y-TZP surface and corresponding countermeasures

After ultrasonic cleaning, the machined Y-TZP surface was dark gray. Darkening of Y-TZP irradiated by a nanosecond laser should be a result of oxygen vacancies that were generated at high temperatures due to the release of oxygen atoms after substoichiometric dioxide formation, in which ZrO_2 became ZrO_{2-X}[4,15]. Noda *et al.* reported that a surface irradiated by a Nd:YAG laser became darkened and that the oxygen concentration clearly decreased, whereas the zirconium concentration increased[7]. Irradiated Y-TZP disks heated at 1,000°C for 5 min in air retuned to their original white color. Applying the above reduction reaction to the present study, Y-TZP was heated in the atmosphere to reabsorb oxygen. After heating, the Y-TZP became white again. The high temperature allows oxygen to diffuse back to vacancies in the irradiated surface, rebuilding the crystalline structure and recovering the white color of Y-TZP. This heating is thought not to have an adverse clinical effect because the porcelain is sintered on Y-TZP at higher than 1,000°C. Matysiak *et al.* reported a similar result in which blackening occurred within holes on zirconia irradiated using a HeNe laser[16]. After heating at 1,350°C, the sample became white again, and there was no significant variation after the heat treatment. The recovery of the white color of the surface enables the fabrication of esthetic dental prostheses without opaquing using Y-TZP machined with a Nd:YVO_4 laser. The effect of the nanosecond laser on the machined Y-TZP surface was small, and we assume that the mechanical properties will not be adversely affected to a significant degree.

Future development

The primary problems associated with the laser machining of Y-TZP reported herein are a long machining time and high cost. Fabrication of the inner surface of the Y-TZP coping required approximately eight hours. However, sintering a partially sintered zirconia coping fabricated by a CAD/CAM system requires up to 18 h. Moreover, the long machining time required when using the laser can be shortened by using a prefabricated coping of fully sintered Y-TZP.

A nanosecond laser machine that can machine a high-thermal-expansion, low-thermal-conductivity material, such as Y-TZP, will also be able to machine other dental materials, such as resins and metals. If the machine is miniaturized and becomes widely used, the cost may be reduced considerably.

The toughness and high strength of Y-TZP are similar to the characteristics of metallic materials. For this reason, Y-TZP has been used in numerous applications in which previously only metals were believed to be suitable, such as moving parts of engines, valve components, milling and cutting tools, wire-drawing dies, and scissors[8]. Y-TZP is also a popular material for use in bio-medical applications due to its outstanding mechanical properties, reliability, and excellent biocompatibility. The ability to carry out accurate laser machining of Y-TZP would allow its properties to be more widely exploited, in particular for applications in which uniquely shaped, intricately structured components are required, not only in industry but also in dentistry.

CONCLUSIONS

A Y-TZP coping was fabricated using a CAD/CAM system in which a partially sintered Y-TZP block was milled and subsequently sintered in a furnace, because fully sintered Y-TZP is too difficult to machine using milling techniques. Furthermore, the design compensates for the volume shrinkage that occurs during sintering of Y-TZP blocks. Thus, we devised a new method by which to machine Y-TZP copings using an industrial Nd:YVO_4 Q-switched nanosecond laser. The following conclusions were obtained based on the results of the present study.

1. An average power of 7.5 W was determined to be the optimal lasing condition because this condition provided the smoothest surface with high machining efficiency.
2. The convergence angle of the inner coping obtained at the first machining did not adequately agree with the provided machining 3D-CAD data. At the fourth machining, however, the convergence angle of the inner coping was 10.9° (SD=0.18°), which is approximately the same as the provided machining 3D-CAD data.
3. The dimensional difference in the height direction was at most 132 μm (SD=59 μm), and the dimensional difference in the width direction at the fourth machining was at most 20 μm (SD=2.4 μm).
4. The machined copings fit accurately on the metal die.
5. The proposed method using a nanosecond Nd:YVO_4 laser machine was demonstrated to be useful for fabricating a coping directly from fully sintered Y-TZP.

REFERENCES

1) Rosenstiel SF, Land MF, Fujimoto J. Contemporary fixed prosthodontics. 3rd ed. St. Louis: Mosby; 2001; p.262-271.
2) Conrad HJ, Seong WJ, Pesun IJ. Current ceramic materials and systems with clinical recommendations: A systematic review. J Prosthet Dent 2007; 98: 389-404.
3) Sjogren G, Lantto R, Granberg A, Sundstrom BO, Tillberg A. Clinical examination of leucite-reinforced glass-ceramic crowns (Empress) in general practice: a retrospective study. Int J Prosthodont 1999; 12:122-128.
4) Beuera F, Aggstaller H, Edelhoff D, Gernet W, Sorensen J. Marginal and internal fits of fixed dental prostheses zirconia retainers. Dent Mater 2009; 25: 94-102.
5) Denry I, Holloway JA. Ceramics for dental applications: A review. Materials 2010; 3: 351-368.
6) Yamagishi T, Ito M, Fujimura Y. Mechanical properties of laser welds of titanium in dentistry by pulsed Nd:YAG laser apparatus. J Prosthet Dent 1993; 70: 264-273.
7) Noda M, Okuda Y, Tsuruki J, Minesaki Y, Takenouchi Y, Ban S. Surface damages of zirconia by Nd:YAG dental laser irradiation. Dent Mater J 2010; 29: 536-541.
8) Wang X, Shephard JD, Dear FC, Hand DP. Optimized nanosecond pulsed laser micromachining of Y-TZP ceramics. J Am Ceram Soc 2008; 91: 391-397.
9) McLean JW, von Fraunhofer JA. The estimation of cement film thickness by an in vivo technique. Br Dent J 1971; 131: 107-111.
10) Vagkopoulou T, Koutayas SO, Koidis P, Strub JR. Zirconia in dentistry: Part 1. Discovering the nature of an upcoming bioceramic. Eur J Esthet Dent 2009; 4: 130-151.
11) Erkorkmaza K, Alzaydia A, Elfizyb A, Enginb S. Time-optimal trajectory generation for 5-axis on-the-fly laser drilling. CIRP ANN 2011; 60: 411-414.
12) Campanelli SL, Casalino G, Ludovico AD, Bonserio C. An artificial neural network approach for the control of the laser milling process. Int J Adv Manuf Technol 2013; 66: 1777-1784.
13) Friel GJ, Conroy RS, Kemp AJ, Sinclair BD, Ley JM. Q-switching of a diode-pumped Nd:YVO_4 laser using a quadrupole electro-optic deflector. Appl Phys B 1998; 67: 267-270.
14) Yoshioka S, Kobayashi T, Tanaka Y, Yamamoto Y, Miyazaki T. Blackening and crack formation in Q-switched YAG laser machining of zirconia ceramics. J Jpn Soc Prec Eng 1989; 55: 1277-1282.
15) Janek J, Korte C. Electrochemical blackening of yttria-stabilized zirconia–morphological instability of the moving reaction front. Solid State Ionics 1999; 116: 181-195.
16) Matysiak M, Parry JP, Crowder JG, Hand DP, Shephard JD, Jones N, Jonas K, Weston N. Development of optical techniques for noncontact inspection of Y-TZP parts. Int J Appl Ceram Technol 2011; 8: 140-151.

Ⅲ．研究成果の刊行に関する資料④

J. Biomed. Mater. Res. Part B, 102B:721-728 (2014)

Society For Biomaterials

Screening study on hemolysis suppression effect of an alternative plasticizer for the development of a novel blood container made of polyvinyl chloride

Yuji Haishima,[1]* Tsuyoshi Kawakami,[2] Chie Hasegawa,[1] Akito Tanoue,[3] Toshiyasu Yuba,[4] Kazuo Isama,[2] Atsuko Matsuoka,[1] Shingo Niimi[1]

[1]Division of Medical Devices, National Institute of Health Sciences, 1-18-1 Kamiyoga, Setagaya-ku, Tokyo 158-8501, Japan
[2]Division of Environmental Chemistry, National Institute of Health Sciences, 1-18-1 Kamiyoga, Setagaya-ku, Tokyo 158-8501, Japan
[3]Department of Pharmacology, National Center for Child Health and Development, 2-10-1 Okura, Setagaya-ku, Tokyo 157-8535, Japan
[4]Corporate Research and Development Division, Kawasumi Laboratories, INC., Shinagawa Intercity Tower B, 9th Floor 2-15-2, Konan, Minato-ku, Tokyo 108-6109, Japan

Received 20 June 2013; revised 2 September 2013; accepted 22 September 2013
Published online 24 October 2013 in Wiley Online Library (wileyonlinelibrary.com). DOI: 10.1002/jbm.b.33052

Abstract: The aim of this study is to identify a plasticizer that is effective in the suppression of the autohemolysis of the stored blood and can be used to replace di(2-ethylhexyl) phthalate (DEHP) in blood containers. The results of hemolysis test using mannitol-adenine-phosphate/red cell concentrates (MAP/RCC) spiked with plasticizers included phthalate, phthalate-like, trimeliate, citrate, and adipate derivatives revealed that di-isononyl-cyclohexane-1,2-dicarboxylate (Hexamoll® DINCH), di(2-ethylhexyl)-1,2,3,6-tetrahydro-phthalate (DOTP), and diisodecyl phthalate (DIDP) exhibited a hemolysis suppression effect almost equal to that of DEHP, but not other plasticizers. This finding suggested that the presence of 2 carboxy-ester groups at the *ortho* position on a 6-membered ring of carbon atoms may be required to exhibit such an effect. The hemolytic ratios of MAP/RCC-soaked polyvinyl chloride (PVC) sheets containing DEHP or different amounts of DINCH or DOTP were reduced to 10.9%, 9.2–12.4%, and 5.2–7.8%, respectively (MAP/RCC alone, 28.2%) after 10 weeks of incubation. The amount of plasticizer eluted from the PVC sheet was 53.1, 26.1–36.5, and 78.4–150 μg/mL for DEHP, DINCH, and DOTP, respectively. PVC sheets spiked with DIDP did not suppress the hemolysis induced by MAP/RCC because of low leachability (4.8–6.0 μg/mL). These results suggested that a specific structure of the plasticizer and the concentrations of least more than ~10 μg/mL were required to suppress hemolysis due to MAP/RCC. © 2013 Wiley Periodicals, Inc. J Biomed Mater Res Part B: Appl Biomater, 102B: 721–728, 2014.

Key Words: DEHP, alternative plasticizer, hemolysis, blood container, PVC medical device

How to cite this article: Haishima Y, Kawakami T, Hasegawa C, Tanoue A, Yuba T, Isama K, Matsuoka A, Niimi S. 2014. Screening study on hemolysis suppression effect of an alternative plasticizer for the development of a novel blood container made of polyvinyl chloride. J Biomed Mater Res Part B 2014:102B:721–728.

INTRODUCTION

Phthalate esters, particularly di(2-ethylhexyl) phthalate (DEHP), have been extensively used as plasticizers due to their ability to increase the flexibility of polyvinyl chloride (PVC), a plastic polymer used in a wide array of products, including medical devices such as tubing, intravenous bags, blood containers, and catheters. DEHP is easily eluted from PVC products into food, pharmaceuticals, and body fluids that touch the plastic, causing the migration of DEHP directly and/or indirectly into the human body.[1,2]

Some phthalates, including DEHP, are considered toxic because they exhibit effects in young rodents that are similar to the antiandrogenic effects of endocrine disruptors in male rats, wherein alterations in the development of the male reproductive system and production of normal sperm are observed.[3–5] Mono(2-ethylhexyl) phthalate (MEHP) is an active metabolite of DEHP and suggested that the toxic effects of orally ingested DEHP are likely caused by the corresponding monoester, and not by the intact DEHP.[6–9] Although the *in vivo* reproductive and developmental toxicity of DEHP in the human body are not yet well understood, recent *in vitro* toxicological studies using human cells have reported that MEHP causes adverse effects such as reduction in the number of germ cells by increasing their apoptosis without altering their proliferation.[10–12] Therefore, precautions should be taken to limit human exposure to

Correspondence to: Y. Haishima (e-mail: haishima@nihs.go.jp)

MEHP, particularly in the case of high-risk patients such as male neonates, male fetuses, and peripubertal male individuals.

The use of plasticizers other than DEHP is an option for developing safer PVC products for human use. PVC medical devices that use trioctyl trimellitate (TOTM), di-isononyl-cyclohexane-1,2-dicarboxylate (Hexamoll® DINCH),[13,14] or acetyl tributyl citrate (ATBC) instead of DEHP have already been developed and are commercially available. Several agencies and official organizations worldwide have individually evaluated the safety of DEHP released from PVC products. Recently, regulation of the use of DEHP has been tightened worldwide, particularly in Europe, not only for toys, childcare products, food apparatus, containers, and packages but also for medical devices. In many countries, including USA, Canada, and Japan, the use of alternative plasticizers to develop safer PVC products and a switch to other plastic products have been recommended for the medical treatment of high-risk patients. However, the use of PVC blood bags containing DEHP has been permitted in Japan without any regulation other than storage at low temperatures because DEHP has been found to be effective in preserving stored red blood cells (RBCs).[15]

We recently developed a prototype of a novel and biologically safer blood container consisting of UV-irradiated PVC sheets[16] from which the elution of DEHP was almost suppressed. On evaluating the safety of the prototype, we found that the hemolytic ratio of the heparinized bovine blood stocked in the container was lower than that of the blood stored in normal PVC blood bags (data not shown). It has also been reported that under periodic mixing conditions, DINCH-PVC bags exhibit protective effects against RBC hemolysis almost identical to that of normal DEHP-PVC containers.[17] These findings suggested that the ability of DEHP to prevent hemolysis must be reviewed and that some plasticizers other than DEHP may also suppress hemolysis. In the present study, we estimated the ability of multiple plasticizers to suppress hemolysis and examined the relationship between the degree of the prevention effect and the amount of plasticizer eluted from the PVC sheets as a preliminary screening in order to identify a candidate for the replacement of DEHP in RBC storage bags.

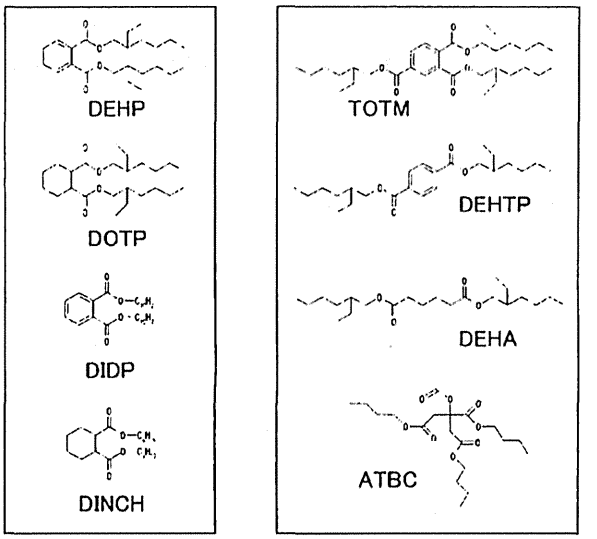

FIGURE 1. Chemical structures of the plasticizers used in this study. The iso-nonyl side-chain of DINCH consists of ~10% n-nonyl, 35–40% methyloctyl, 40–45% dimethylheptyl, and 5–10% methylethylhexyl isoforms. DIDP contains an isometric mixture of phthalates with primary C10 branched dialkyl chains.

MATERIALS AND METHODS

Materials, chemicals, and utensils

Eight kinds of plasticizers were used in this study (Figure 1). TOTM, ATBC, diisodecyl phthalate (DIDP), di(2-ethylhexyl)-1,2,3,6-tetrahydro-phthalate (DOTP), bis(2-ethylhexyl) terephthalate (DEHTP), di(2-ethylhexyl) adipate (DEHA), and epoxidized soybean oil (ESBO) were purchased from Tokyo Chemical Industry Co. Ltd. (Tokyo, Japan). Hexamoll® DINCH was provided by BASF (Ludwigshafen, Germany). DEHP, DEHP-d_4, diethyl ether of pesticide residue and PCB analysis grade, and phthalate-analytical-grade hexane were purchased from Kanto Chemical (Tokyo, Japan). Sodium chloride of pesticide residue and PCB analysis grade and phthalate-analytical-grade anhydrous sodium sulfate were purchased from Wako Pure Chemical Industries, (Tokyo, Japan) and ultrapure water obtained using Milli-Q Synthesis A10 (Millipore, Tokyo, Japan) were used to prepare the sample for gas chromatography/tandem mass spectroscopy (GC-MS/MS) analysis. Heparin sodium was purchased from the Society of Japanese Pharmacopoeia (Tokyo, Japan), and other chemicals were purchased from Wako Pure Chemical Industries. All the utensils made of glass, metal, or Teflon® were heated at 250°C for more than 16 h prior to use.

Preparation of heparinized blood and MAP/RCC

Human blood (total of 200 mL) was obtained from a volunteer at our own laboratory. The procedure was performed in accordance with the ethical guidelines of the National Institute of Health Sciences (approval number 188). The blood was immediately mixed at 4°C with heparin (2000 units) or citrate-phosphate-dextrose (CPD) solution (28 mL) consisting of sodium citrate hydrate (26.3 g/L), citric acid hydrate (3.27 g/L), glucose (23.2 g/L), and sodium dihydrogen phosphate (2.51 g/L). The heparinized blood (Htc, 43%) was stocked at 4°C until use. The blood mixed with the CPD solution was centrifuged at 3000*g* for 10 min at 4°C followed by removal of the upper layer. Mannitol-adenine-phosphate (MAP) solution (46 mL) consisting of D-mannitol (14.57 g/L), adenine (0.14 g/L), sodium dihydrogen phosphate (0.94 g/L), sodium citrate hydrate (1.5 g/L), citric acid hydrate (0.2 g/L), glucose (7.21 g/L), and sodium chloride (4.97 g/L) was added to the remaining RCC layer to prepare MAP/RCC (Htc. 59%), and the solution was stocked at 4°C until use.

Preparation of PVC sheets

The PVC powder (100 g) was gradually added to the mixture of DEHP (55 g) and ESBO (8 g) while stirring with a spatula. The mixed powder was gently heated from room temperature to 100°C in an oven and then stirred well. The powder was stirred a second time after heating at 100°C for 5 min to completely plasticize PVC. The plasticized powder was heat-pressed at 180°C to prepare the PVC sheets (thickness = 0.4 mm; final DEHP concentration = 33.7 w/w%). The PVC powder was also plasticized in the presence of TOTM (85 g; final concentration = 44.0 w/w%), different amounts of DINCH, DIDP, or DOTP (35, 60, 85, and 110 g, respectively; final concentration = 24.5, 35.7, 44.0, and 50.5 w/w%, respectively), instead of DEHP, and then heat-pressed using the same method. Each sheet was cut into small pieces (3.2 × 1 cm).

Hemolysis test

Each plasticizer was dissolved in suitable amounts of diethyl ether, which was placed into a screw-capped glass bottle. After drying on a clean bench overnight without the bottle cap, 5 mL of heparinized blood or MAP/RCC freshly prepared was added to the bottle (final concentration: 1 or 100 μg/mL, respectively). Additionally, each PVC sheet (3.2 × 1 cm, thickness = 0.4 mm) containing different kinds and amounts of plasticizers was placed into a screw-capped glass bottle, and 5 mL of freshly prepared MAP/RCC was added to the bottle.

During incubation at 4°C for 35 days in the case of heparinized blood or 10 weeks in the case of MAP/RCC under continuous gentle shaking, an aliquot (50 μL) of the blood sample was collected into Eppendorf tubes every week. PBS (1 mL) was added to each sample and gently mixed, followed by centrifugation at 500 × *g* for 2 min at 4°C, and then the absorbance of the supernatant (100 μL) was measured at 415 nm with a SH-9000 Lab microplate reader (Corona Electric, Ibaraki, Japan). Heparinized blood or MAP/RCC alone was also tested under the same conditions as the negative control, while the positive control was prepared by adding distilled water instead of PBS. This test was repeated in triplicate, and the significant difference was calculated by two-way analysis of variance (ANOVA). The hemolytic ratio was calculated in accordance with the following formula.

$$\% \text{ Hemolysis} = (A_T - A_N)/(A_P - A_N) \times 100$$

A_T: Test sample absorbance, A_N: Average negative control mean absorbance, A_P: Average positive control mean absorbance

Elution test for the plasticizer

The quantity of plasticizer in each PVC sheet soaked with the blood samples was measured according to a previously reported method.[18-20] Briefly, an aliquot (50 μL) of MAP/RCC sample for the hemolysis test was collected into a screw-capped glass tube every week, and sodium chloride (1 mL, 1 w/v%), DEHP-d_4 (0.1 μg), and hexane (1 mL) were added. After shaking vigorously for 15 min and centrifuging at 3000 rpm for 10 min at room temperature, the organic phase was collected and dehydrated with anhydrous sodium sulfate and this was followed by GC-MS/MS analysis, as described below. This test was repeated in triplicate, concomitantly with the hemolysis test. The significant difference was calculated by two-way ANOVA.

GC-MS/MS analysis

The plasticizers in each sample were measured by GC-MS/MS, using a Trace GC with a Quantum XLS (Thermo Fisher Scientific, Waltham, MA) equipped with DB-5MS fused silica capillary column (length: 30 m, internal diameter: 0.25 mm, film thickness: 0.25 μm; Agilent Santa Clara, CA). The carrier gas was He with a flow rate of 1.0 mL/min. The temperature of the injector, transfer line, and ion source were 250°C. The sample (1 μL) was injected in the splitless mode. The GC oven temperature was initially maintained at 60°C for 2 min, and it was increased to 310°C at a rate of 20°C/min. The MS/MS system was operated under the multiple reaction-monitoring mode (MRM) with electron impact ionization (EI: 70 eV). Ar gas was used as the collision gas (0.13 Pa). The retention times, the precursor (Q1) and product (Q2) ions of the plasticizers, and the collision energies of each plasticizer were listed in Table I.

The product ions of all the plasticizers were used for quantification that was performed using DEHP-d_4 as the internal standard. The concentrations of DINCH and DIDP were determined using the sum of the total peak area of their isomers, similar to a previous study.[21] The limits of detection and quantification (LOD and LOQ, respectively)

TABLE I. Retention Times, Precursor Ions (Q_1), Product Ions (Q_2), Colligion Energies, LODs, LOQs, Recoveries, and its Coefficients of Variation (CV) of the Target Chemicals.

Chemicals	Retention Time (min)	Q_1 [m/z]	Q_2 [m/z]	Collision Energy (V)	LOD[a] (ng/mL)	LOQ[a] (ng/mL)	Recovery[b] (%)	CV (%)
DOTP	14.34	170	124	7	0.12	0.39	101	2.8
DEHP	14.54	167	149	4	0.051	0.17	99	1.5
DINCH	14.60-16.60	155	109	5	0.45	1.5	101	1.8
DIDP	15.60-17.60	307	149	13	0.64	2.1	109	5.5
TOTM	20.97	305	193	16	0.040	0.13	123	7.1
DEHP-d_4[c]	14.53	171	153	4				

[a] Calculated by TOCO version 2.0 (FUMI theory). The values correspond to the concentration in the injected solution.
[b] Adding every compound to the blood sample (10 μg/mL, n = 5).
[c] Internal standard.

were calculated using total optimization of chemical operations (TOCO) software version 2.0 and the function of mutual information (FUMI) theory.[22] The concentrations obtained using the relative standard deviations of 33% and 10% on the basis of the mass chromatograms of the standard and blank solutions, respectively, were used as the instrumental LOD and LOQ. The recovery test was conducted by adding every compound to the blood sample (10μg/mL, n=5). The blank test was conducted using the blood sample without PVC sheets. Only DEHP was detected under the LOQ level.

RESULTS

Identification of an alternative plasticizer effective in suppressing hemolysis

First, we estimated whether the plasticizer itself exhibited the suppression effect on hemolysis. As shown in Figure 2, the hemolytic ratio of the heparinized blood in the absence of plasticizers increased in a time-dependent manner and reached 61.6% after 35 days of incubation (control). The hemolysis behavior of the heparinized blood spiked with each plasticizer was similar to that of the control or was slightly higher, indicating that all the plasticizers were ineffective in suppressing hemolysis irrespective of the type and amount spiked. Although all the plasticizers did not exhibit hemolysis suppression against MAP/RCC at the concentration of 1 μg/mL [Figures 3(a,b)], the hemolytic ratio of MAP/RCC spiked with DINCH, DIDP, or DOTP at the dose of 100 μg/mL significantly decreased to 10.3%, 12.1%, and 9.5%, respectively, in comparison with the ratio of MAP/RCC containing no additives, which reached 18.9% after 10 weeks of incubation [Figure 3(c)]. The degree of the effect of the plasticizers was almost identical to that of DEHP (hemolysis ratio = 10.9% after 10 weeks of incubation). Additionally, TOTM, ATBC, DEHTP, and DEHA did not suppress the hemolysis of MAP/RCC even at the concentration of 100 μg/mL [Figure 3(d)].

Hemolysis suppression by the PVC sheet containing plasticizer

Similar to the result of the first screening, PVC sheets spiked with different amounts of DINCH, DIDP, or DOTP were prepared, and their hemolysis suppression effect against MAP/RCC was estimated. The size of the PVC sheet and the amount of MAP/RCC used in this study were decided based on the ratio between the inner surface area and the blood volume of the typical RBC storage bags (KARMI Blood Bag KBQ-200AML, Kawasumi Laboratories, INC., Tokyo, Japan). The PVC sheets spiked with DEHP or TOTM were used as the positive or negative control, respectively.

As shown in Figure 4(a), the hemolytic ratio of MAP/RCC in the absence of the PVC sheets increased in a time-dependent manner and reached 29.4% after 10 weeks of

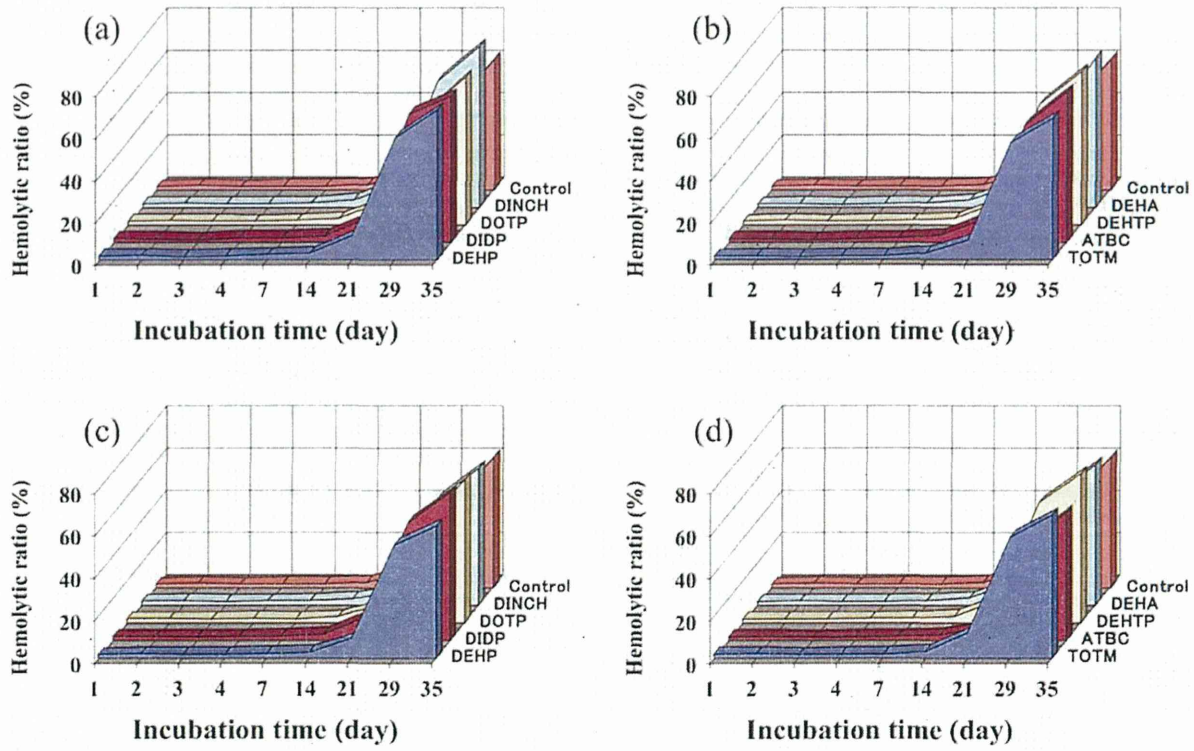

FIGURE 2. Hemolytic behavior of heparinized blood containing plasticizers at the concentration of 1 μg/mL (a, b) or 100 μg/mL (c, d). No significant difference was detected between the control and each plasticizer irrespective of the type and amount spiked. [Color figure can be viewed in the online issue, which is available at wileyonlinelibrary.com.]

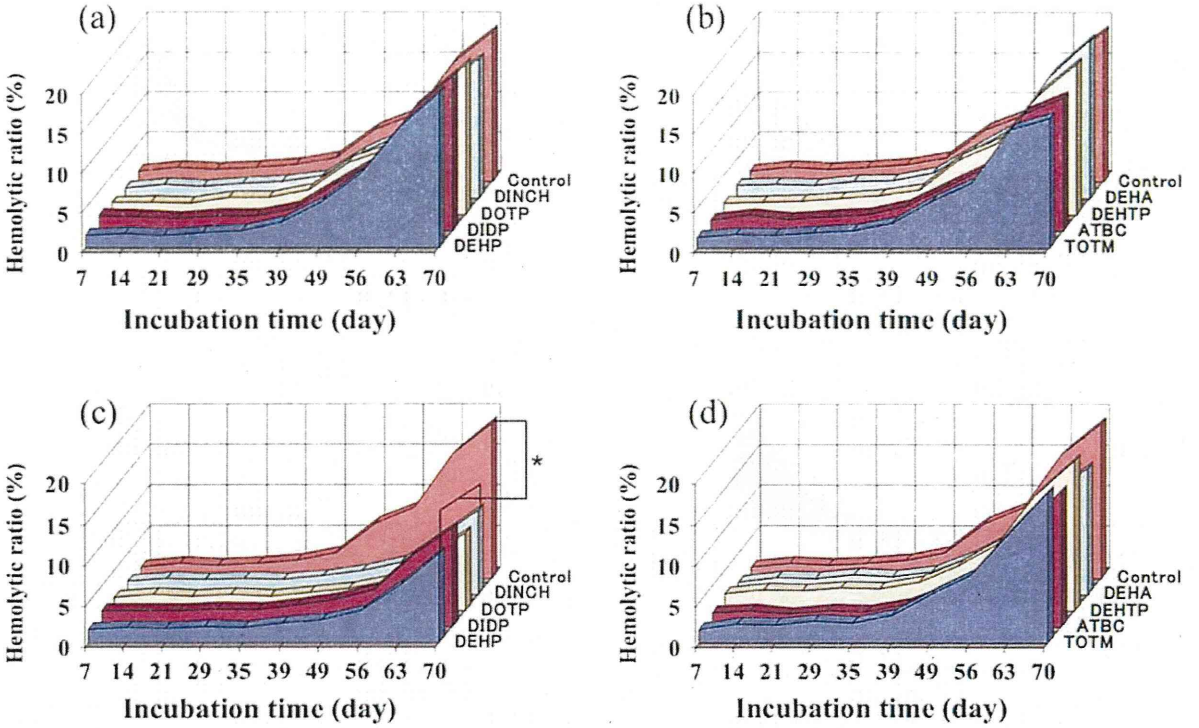

FIGURE 3. Hemolytic behavior of MAP/RCC containing plasticizers at the concentration of 1 μg/mL (a, b) or 100 μg/mL (c, d). *Significant difference ($p < 0.05$) was detected between the control and plasticizers, such as DEHP, DIDP, DOTP, and DINCH, effective in suppressing hemolysis at the concentration of 100 μg/mL (c), but not among these four plasticizers. [Color figure can be viewed in the online issue, which is available at wileyonlinelibrary.com.]

incubation. The hemolytic behavior of MAP/RCC in the presence of the PVC sheet containing TOTM (50.5%) was almost identical, and the ratio reached 28.2% after incubation [Figure 4(a)]. The PVC sheets spiked with DEHP (33.7 w/w%), DINCH (24.5–50.5 w/w%), or DOTP (24.5–50.5 w/w%) considerably decreased the hemolytic ratio to 10.9%, 9.2–12.4%, and 5.2–7.8%, respectively [Figure 4(a–c)]. The degree of hemolysis suppression effect of the PVC sheets containing DINCH or DOTP was not greatly influenced by the difference in the plasticizer content. Although DIDP itself had the ability to suppress hemolysis of MAP/RCC, the PVC sheet containing DIDP (24.5–50.5 w/w%) did not exhibit a significant hemolysis suppression effect, irrespective of the amounts spiked [Figure 4(d)].

Plasticizer elution test

The elution of the plasticizers from the PVC sheets containing DEHP, TOTM, DINCH, DIDP, or DOTP was determined to evaluate the relationship between the degree of the hemolysis suppression effect against MAP/RCC and the amount of plasticizer released from each PVC sheet. These plasticizers were quantified by GC-MS/MS analysis by using DEHP-d_4 as the internal standard. The LOD, LOQ, and recovery values are listed in Table I.

As shown in Table II, the amount of DEHP released from the PVC sheet spiked with DEHP (33.7 w/w%) increased in a time-dependent manner and reached 53.1 ± 6.07 μg/mL after 10-week incubation in MAP/RCC. The amount of plasticizer eluted from the PVC sheet containing TOTM (50.5%) was significantly low, corresponding to only 0.27 ± 0.09 μg/mL even after the 10 week incubation. The amount of plasticizer eluted from the PVC sheet spiked with DOTP (24.5, 35.7, 44.0, and 50.5 w/w%) increased in a time- and dose-dependent manner. The amount was approximately 2–3 times greater than that of DEHP and reached 78.4 ± 13.7, 117 ± 8.0, 143 ± 16.8, and 150 ± 26.0 μg/mL, respectively, after 10 weeks of incubation. The amounts of DINCH and DIDP released from the PVC sheets containing each plasticizer (24.5, 35.7, 44.0, and 50.5 w/w%) also increased in a time-dependent manner and reached 26.1–36.5 and 4.80–5.96 μg/mL, respectively. However, a significant difference was not clearly detected in the amount of elution in response to the plasticizer content. The degree of elution of DIDP was ~10 times lower than that of DEHP, irrespective of the amounts spiked. The amount of elution of DINCH was also lower than that of DEHP.

DISCUSSION

This screening study investigated alternative plasticizers exhibiting a hemolysis suppression effect against RBCs and evaluated the relationship between the degree of the suppression effect and the amount of the plasticizer eluted

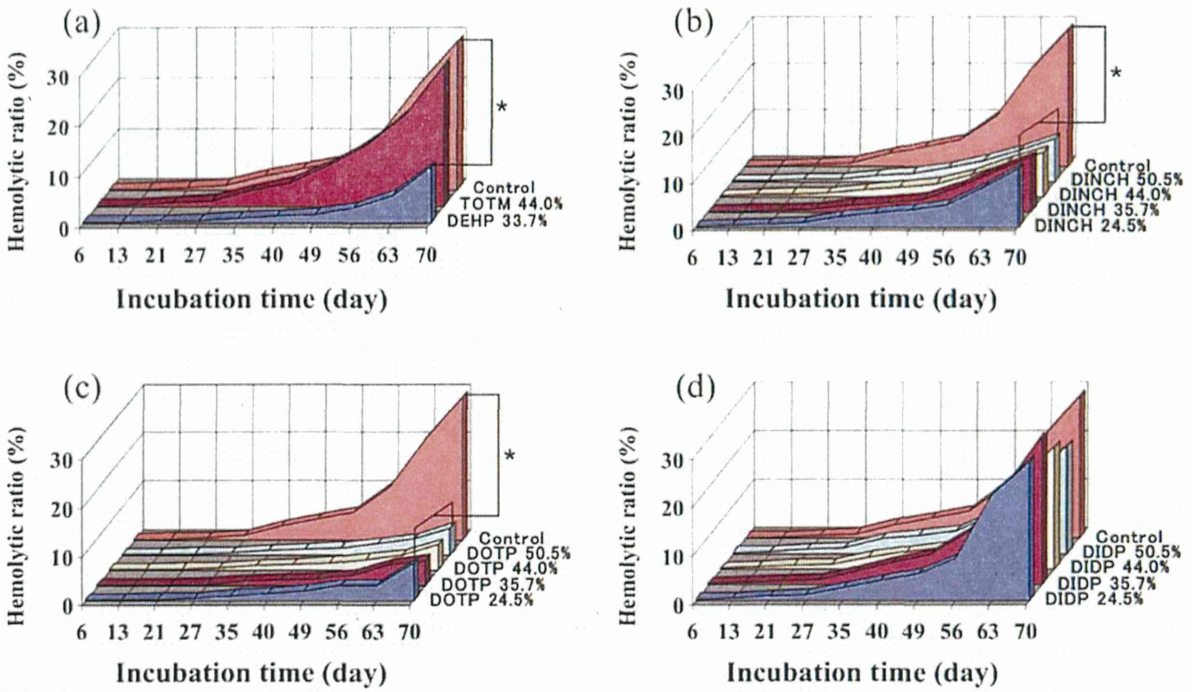

FIGURE 4. Hemolytic behavior of MAP/RCC in the presence of PVC sheets spiked with several plasticizers. (a) No plasticizer (control); DEHP (33.7 w/w%); and TOTM (44.0 w/w%). (b) DINCH (24.5, 35.7, 44.0, and 50.5 w/w%). (c) DOTP (24.5, 35.7, 44.0, and 50.5 w/w%). (d) DIDP (24.5, 35.7, 44.0, and 50.5 w/w%). *Significant difference ($p < 0.01$) was detected between the control and DEHP (a), and control and DINCH (b) or DOTP (c), while there was no significant difference between the control and DIDP. [Color figure can be viewed in the online issue, which is available at wileyonlinelibrary.com.]

from the PVC sheet. The chemical structures of the plasticizers used in this study are shown in Figure 1. The results of the hemolysis test, in which 8 kinds of plasticizers structurally categorized into five groups were used, suggested that the presence of 2 carboxy-ester groups at the *ortho* position on a 6-membered ring of carbon atoms may be needed for the plasticizer to exhibit the effect. DEHP, DIDP, DINCH, and DOTP, all of which have the ability to suppress the hemolysis of MAP/RCC, have such a structure. TOTM possesses this basic structure as a part of the molecule, but its 6-membered ring is substituted by an additional carboxy-ester group, and this might be the reason why TOTM seems to be ineffective in suppressing hemolysis. The same basic structure is not present in DEHTP, DEHA, and ATBC, which did not exhibit any hemolysis suppression effect on MAP/RCC. The structure of the 6-membered ring does not seem to be restricted to aromatic compounds because the suppression effect is also seen in the case of partially unsaturated or saturated rings. The mechanism underlying hemolysis suppression by DEHP, DINCH, DIDP, and DOTP is unknown, but it could be speculated that these plasticizers may be incorporated into and stabilize the lipid bilayer of the RBC membrane, because there is a possibility that plasticizer molecules having the two carboxy-ester groups oriented to the same direction of the *ortho* position may form a pair at the inner and outer sides of the RBC membrane and act as one component of the lipid bilayer. On the other hand, in case the orientation of the acyl groups is different from each other, the plasticizer molecules may be also incorporated into the lipid bilayer, but not form such a pair. The results suggested that the degree of hemolysis suppression effect is due in part to the concentration of the plasticizer eluted, but also to the structurally intrinsic ability of the plasticizer molecule. However, since the degree of the effect of PVC sheets containing DINCH or DOTP was not greatly influenced by the differences in the plasticizer content, the effect is saturated at a certain concentration. As shown in Figure 4, the hemolysis suppression effect induced by the PVC sheet spiked with DEHP, DINCH, or DOTP appeared after 35 days of incubation. The minimum amounts of these plasticizers eluted from each PVC sheet during the incubation period were 34.7 (DEHP), 13.5 (DINCH), and 61.3 (DOTP) μg/mL, respectively, while the maximum elution amount of DIDP was only 2.94 μg/mL (Table II). Taking these results into consideration, the use of plasticizer at a concentration of least more than ~10 μg/mL seems to be necessary to protect RBCs from hemolysis because the PVC sheet spiked with DIDP did not significantly prevent the hemolysis of MAP/RCC. It has been reported that the leachability of TOTM, DINCH, and diisononyl phthalate (DINP) from PVC products is significantly lower than that of DEHP.[23,24] The reason for this phenomenon is still unknown, but it could be speculated that the degree of intermolecular interactions and/or steric hindrance between the PVC and